ASME Journal of Solar Energy Engineering
Online journal at:
https://asmedigitalcollection.asme.org/solarenergyengineering

Kenneth M. Armijo[1]
Sandia National Laboratories,
P.O. Box 5800,
Albuquerque, NM 87185
e-mail: kmarmij@sandia.gov

Matthew Muller
National Renewable Energy Laboratory,
15013 Denver West Parkway,
Golden, CO 80401
e-mail: matthew.muller@nrel.gov

Daniel Tsvankin
National Renewable Energy Laboratory,
15013 Denver West Parkway,
Golden, CO 80401
e-mail: daniel.tsvankin@nrel.gov

Dimitri Madden
Sandia National Laboratories,
P.O. Box 5800,
Albuquerque, NM 87185
e-mail: damadde@sandia.gov

Review and Gap Analysis of Heliostat Components and Controls

This investigation provides a comprehensive literature review pertaining to heliostat components and controls as part of the U.S. Department of Energy (DOE), Heliostat Consortium (Heliocon) program. This work presents a detailed assessment of subcomponents, controls and wireless communications elements that comprise various designs of helisotats within concentrating solar power (CSP) installations. Additionally, this work also provides the results of an industry survey, intended to compliment the literature discussion, to provide a gap analysis of the primary technology and cost areas that need to be addressed to help improved to spur concentrating solar power (CSP) bankability. Although the results of the study determined several key areas for development, three strategic areas identified were: (1) the use of advanced composite materials to replace a need for expensive steel within the structure and mirror substrate, (2) employment of closed-loop controls for automated calibration, reduction of commissioning time and O&M hours, reduction of drive requirements, as well as overall cost reduction, and (3) the need for more Heliostat-centric codes and standards to facilitate engineering confidence in the development of new features, cost reductions, or other design iterations to be seamlessly introduced without optical performance problems. [DOI: 10.1115/1.4065976]

Keywords: heliostats, collector, concentrating solar power, system controls

1 Introduction

Heliostats assemblies are device assemblies that operate within a highly controlled manner to provide accurate solar radiation during concentrating solar power (CSP) operation. General composition includes a reflective area, control system, and a mounting and tracking mechanism. A reflective area is typically made up of one or more mirrors (also called facets), with a surface area that, on some heliostats, has reached 178.5 m^2 [1]. According to Coventry and Pye [2], Gen 1 and 2 heliostats have a size range of 1.14 m^2 (eSolar) to 120 m^2 (Abengoa), with various sizes in between, e.g., 15.2 m^2 (BrightSource), 62.5 m^2 (Pratt & Whitney), and 116 m^2 (Sener) [3–7]. These efforts have required optimization of the component designs to lower costs of customized components (such as the drive system, which can account for up to 30% of total cost, primarily for the azimuth drive [8]).

The kinematic design of a heliostat can also vary based on different actuation styles. The following are general designs used for motion control:

- Azimuth-elevation
  - This is the most common setup in grid-scale CSP plants. This axis arrangement results in a T-shaped heliostat. The primary axis of rotation is azimuthal (about a vertical axis). The secondary axis of rotation is elevation (about a horizontal axis) using a torque tube. This section typically refers to heliostat components (e.g., pedestals, azimuth drives) in context of an azimuth-elevation heliostat.
  - Some azimuth-elevation heliostats are able to eschew a traditional azimuth drive for a large carousel at their base.
  - Some heliostats that utilize slope drives to allow the usage of linear actuators for both tracking axes. This allows to lower heliostat drive costs overall by eliminating the need for more expensive slew drives.
- Horizontal first (elevation-azimuth)
  - This setup uses a primary elevation and secondary azimuthal axis. Both the German Aerospace Center (DLR) and Commonwealth Scientific and Industrial Research Organization (CSIRO) have experimental heliostats that use rim drives to accomplish this style of actuation.
- Target aligned
  - One axis of rotation forms a line from the heliostat to the receiver. The secondary axis runs perpendicular to this one. Heliosystems' PATH heliostat uses this control scheme.
- Swiveled
  - The mirror surface is fixed by a U-joint at one point and actuated at two others. This eliminates primary and secondary rotational axes in favor of combined translation/rotation of the mirror surface plane.

To further improve optics while increasing heliostat surface area, curved facets were introduced [9]. However, larger reflective

[1]Corresponding author.

Contributed by the Solar Energy Division of ASME for publication in the Journal of Solar Energy Engineering: Including Wind Energy and Building Energy Conservation. Manuscript received September 5, 2023; final manuscript received July 8, 2024; published online November 19, 2024. Assoc. Editor: Guangdong Zhu.

surfaces and their respective supporting structures are exposed to higher wind loads and can have the drawback of increasing optical losses and mechanical stress levels [10]. Therefore, there have been trends to utilize single-facet heliostats to optimize heliostat size with respect to receiver geometry, field layout, and costs.

Additionally, to further reduce these costs, newer materials or designs have been considered, such as sandwich panel mirror facet, polymer reflector subcomponents, and coatings to improve reliability or reduce soiling losses. Regardless of design, maximum wind conditions can dictate choices within heliostat components and controls. Additionally, maximum operating torques of the drive train and stiffness of structure are primary factors that determine the relationship between wind speed and performance.

Electronic control of the heliostat drive train is required for adjustment of the heliostat structure so it can track sun position to reflect concentrated sunlight toward a receiver. Wireless and closed-loop controls have become increasingly attractive for new installations as they offer potential cost savings and enhanced performance. Heliostat durability and reliability are not well characterized but are of key importance to ensure high performance and safe operation over the designed lifetime. Component degradation, particularly for drives, mirrors, and electronics are also not well documented in literature, but are critical for predicting long-term system performance and planning, as well as financing system O&M.

Various performance design standards are a typical pathway most industries use to ensure durability, reliability, and to achieve expected performance. Some tracking system standards development has taken place for both concentrating solar photovoltaic (PV) [11] and concentrating solar power (CSP) [12,13], but these standards need to be expanded to fully cover the needs for heliostat components and controls. Additionally, a deficiency of accepted CSP heliostat standards prevents the industry from rapidly validating new durable and bankable designs that enable reducing costs and becoming a mature industry.

2 Component Design

2.1 Drives. Heliostat drives represent one of the most expensive components in a heliostat, as demonstrated by the commercialized Stellio drive comprising 22% of the design's total cost [14]. The specific drive and rotational assembly costs associated with this design would account for 57% of SETO's \$50/m^2 cost target for heliostats, demonstrating the need for further cost reduction. Téllez et al. [15] described two common drive types for heliostats: traditional rotary electromagnetic motors and hydraulic actuators. These drives can be used with several different mechanical transmissions for transferring mechanical energy from the drive to azimuth or elevation axes. These transmissions include worm, spur, chain gears, harmonic, capstan, planocentric drives, rack and pinion systems, spindles, and friction wheels. For azimuth drives, high-precision gears with minimum backlash are required, which are often expensive.

There are currently few drive types deployed at the current commercial scale in the field. Of the 15 CSP tower facilities to enter operation worldwide (per SolarPACES' database) since 2013, all but one use a pedestal configuration with an azimuth slew drive and linear actuation for elevation. These projects comprise a wide range of locations and heliostat developers: Ashalim, Israel; Delingha, China; and Calama, Chile (by BrightSource, Cosin Solar, and Abengoa). BrightSource's current two-facet pedestal heliostat design is shown in Fig. 1. Early-construction installations continue this trend: all six underconstruction grid-scale installations use pedestal-type heliostats. This includes sites in Golmud, China (CGDG Qinghai New Energy) and Redstone, South Africa (ACWA Power).

Traditional drives tend to be reliable for CSP heliostat operation, though can be cost prohibitive, and some studies show that integration into the heliostat could be improved. Typically, a heliostat with

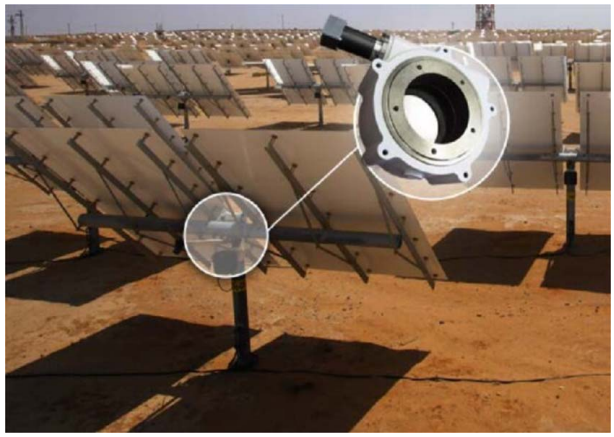

Fig. 1 Typical for current state of the art, the production BrightSource heliostat at Ivanpah uses a worm gear-driven azimuth drive. This particular unit was developed specifically by the firm Cone Drive for BrightSource heliostats. Custom solutions like this must be large scale (which BrightSource can achieve as the heliostat provider for multiple CSP facilities) to be cost-effective. Adapted from Ref. [40].

standard elevation and azimuth control has one linear slope drive for elevation and one slew drive for azimuth. Specifically, azimuth drives responsible for rotating the pedestal about the foundation represent a significant heliostat technology gap. Azimuth drives manufactured by Winsmith have been a previous standard in heliostat design [16]. These drives generally use five gears, one central gear for rotating the pedestal surrounded by three idler gears and one motor-driven gear. The combined five gears are able to achieve a gear reduction for control. However, Winsmith azimuth drives are very expensive. A cost reduction report by Kolb et al. [17] states that for both large and small heliostats, drives are the most expensive component. Drives make up approximately 22% of the cost for large heliostats and up to 57% of the cost for small heliostats. This report also confirms that azimuth drives are typically the most expensive drive type. As stated in the report, conservative or completely alternate designs to the Winsmith drive are needed. Conservative redesigns of the Winsmith azimuth drive may be a solution, as even Winsmith current drives are likely overbuilt, especially on heliostats located in the inner field [18].

A significant problem with the traditional azimuth drive design is the location of the drive at the pedestal top. Prior work by Emes et al. [19] assessed the pedestal and hinge bending moments that occur in unsteady pressure distributions of a turbulent atmosphere. In their study, wind tunnel tests confirmed that turbulence and changing pressure distributions can impose significant moments on the pedestal. Turbulence increases in fields containing a large number of heliostats, which can impact the drive performance of individual heliostats, depending on their relative position within a field. The required pedestal height for optimal performance also increases farther back from a tower as some optimization studies have found [20], which would cause an increased moment on the pedestal base. The height can also be governed by the heliostat chord from not hitting the ground during movement. Overall, excessive loading to pedestal-mounted drives can pose a risk for wear and damage.

Another significant challenge with azimuth drives is complexity. This has pushed many researchers to study alternatives to the standard azimuth drive. A heliostat cost optimization study assessed slew and slope drives as an alternative kinematic system for azimuth control [21] and stated that linear slope drives which use lever arms for azimuth control can provide lower tracking error than traditional azimuth slew drives. Linear slope drives were also stated to be cheaper. As a result, it was found that linear slope drives consistently resulted in a lower the levelized cost of

electricity (LCOE). Free axis arrangements of the slope drive were stated to have additional requirements, however; t-shaped heliostats could have the issue of the corners touching the ground with a linear slope drive, though can be avoided by increasing pedestal height. Pfahl et al. [22] noted that pedestal-mounted slew drives may be more expensive than linear drive systems. Alternate drive systems such as rim drives with cables may also be cheaper than the pedestal mounted systems.

A cost reduction study by Kolb et al. [17] evaluated cost reduction techniques for heliostats where several drive mechanisms were discussed. The study did state that with current understanding of wind loads and torques on heliostat drives, a lower cost drive could easily be used to replace the azimuth drive. The study also mentioned that a lack of production-line manufacturing techniques makes the azimuth drive more expensive than it needs to be. One concept for cost reduction of drives was to use a pipe in pipe azimuth drive, where a pipe rotates within the fixed pedestal to achieve azimuth rotation. This concept has been used at the White Cliffs plant for smaller dishes of approximately 7 m^2 [17] A driving motor at the base of the pedestal rotates the pipe within the pedestal where wind loads are distributed along the length of the pipes rather than on the drive. A 33% cost reduction from conventional azimuth drives was determined feasible with this drive method.

Hydraulic azimuth and elevation drives were discussed for use with relatively large (>60 m^2) heliostats. While large heliostats can be expensive to manufacture and have optical penalties due to worse optical quality, a net cost reduction could still be achieved. Hydraulic drives require more maintenance and are complex but for a large heliostat could offer net cost reduction of \$18/m^2. An analysis of spb's commercially available Stellio heliostat by Potter et al. [21] found that DC electric linear actuators were ultimately responsible for \$16.08/m^2 of the heliostat's ultimate cost, 11.63%. Finally, a water ballasted heliostat motion system was discussed, which would eliminate the need for drives entirely. In this system, water would be pumped between chambers on the back of the facets to change the balance of the heliostat and track the sun. This system would entirely eliminate the need for any gear drives and could bring significant savings.

Various researchers have studied heliostat cost reduction methods with rim drives [22–24]. In a conceptual two rim design, the first rim intersects the pedestal and mounts to a vertical or horizontal support beam. This drive provides changes to the elevation angle. The second rim rests on the first rim and is fixed to the mirror facets to change the azimuth. The drives are designed to be used with winch wheels. In this design, the loads on the drives would be significantly reduced and the long lever arm would allow for the use of low-cost drives. There would be a reduced load on the bearings, mirror panel, and upper pedestal during stow. The energy consumption of the drives would be low as well. However, the drawbacks include increasing the height of the pedestal, which increases the wind load on the base of the pedestal, higher mounting and installation effort requirements, and potentially low stiffness against wind loads in certain mirror panel orientations.

Cable actuation systems are another low-cost alternative to current heliostat drives. One such example is a Google heliostat, which used cable pulley drive systems for elevation and azimuth control [25]. This cable actuation system would require cables to be in constant tension. Google created this condition by mounting the facet panel at the top of a tripod frame. A single U-joint served as the connection between the panel and the tripod frame, acting as a dual hinge which allowed the panel to vary both azimuth and elevation angles. The hinge system was not mounted perfectly centered on the facet panel. Instead, the panel was mounted such that its center of gravity was farther forward than the center of the frame, causing the panel to lean forward. A dual pulley system is then mounted behind the panel with two cables running to the top left and right corners of the panel. The cables pull back on the panel so that it no longer leans forward, keeping the cables perpetually in tension. This system uses an electric pulley winch system to reel in the cables and change the angles of the panel. Pulling both the left and right pulleys at the same time will change the elevation angle. Pulling one cable disproportionately to the other will cause a change in the azimuth angle. In this system, low-cost, low-power motors can be used such as the Google worm drive with anti-backdrive design characteristics that will limit the holding torque requirements of the motor. The use of a cable pulley system such as this would drastically reduce the drive system and motor costs of a heliostat. However, it was noted by Google that their motor pulley system, especially with the low-power motor, would not be able to quickly move the heliostat into a stow position for protection from unexpected high winds or threats to the heliostat.

Drive costs must be reduced, but there are three primary barriers in the process. First, drives are generally overbuilt per current understanding of wind loads. In order to advance alternative low-cost designs or downsize existing drives, research is needed to better characterize high-frequency wind speeds at heliostat heights as well as how wind loading changes throughout a heliostat field design. For small format heliostats, linear drives escape some overbuilding issues though mechanical advantage of off-axis attachment, although other issues (primarily dust and water ingress) exist. Second, the heliostat market volume is too low to support ongoing development and improvement of drives or other components. Current projects must select slew drives or linear actuators that already have volume in other industries.

2.2 Mirrors and Facets. Heliostat facets represent a high proportion of both heliostat component cost and designs that could be improved to reduce LCOE, as well as the levelized cost of heat (LCOH). Commercially available heliostat mirrors (including adhesives and supports) represent \$24/m^2 of the total cost [26]. Most commercially installed heliostats use second-surface mirrors constructed with 3- to 4-mm glass. One exception is Abengoa's ASUP 140 (used in the LuNeng Haixi 50-MW plant), which uses a 2-mm glass reflector. Some variations exist in the means of supporting the reflector. The ASUP 140's relatively thin mirrors are supported by foam in a sandwich-type construction. Material and weight reductions for large heliostats have been achieved by replacing facets' typical solid backing with stamped, lattice-type facet supports. Heliostats installed at Noor III in Morocco (Fig. 2) use this style of construction [1].

Although sandwich- and stamped back sheet-supported facets have been used in commercial installations, further work is needed. The slope error of these facets can reach 0.05 mrad/°C operating deviation from as-manufactured temperature [27]. The Eurostars 2 PHOTON ("High Performance Thermosolar Plants

Fig. 2 Sener's HE54 heliostats at Morocco's Noor III facility (operational since 2018). At 178.5 m^2, this is the largest heliostat in commercial CSP use [1]. Each facet uses a latticed support. This reduces the material usage of the facet itself, a weight reduction which can lower design loads on the drives and heliostat structure. Adapted from Ref. [67].

based on PV-Hybrid Autonomous Heliostats and Tailored Receivers") project has addressed this with thermally balanced sandwich "bi-facets" that reduce this error down to 0.005 mrad/°C, but these are not yet implemented at field scale.

Many parts of mirror and facet design can be improved, ranging from material construction to reliability over a range of environmental conditions. Heliostat mirrors and supports are heavy, adding significant weight to the pedestal, and supports and contributing to heliostat cost. The mirror face of a heliostat acts as a sail in the wind, resulting in the significant wind loads on the pedestal and hinge.

Reducing the load on heliostat components from high wind could significantly reduce overall heliostat cost by reducing structural design requirements. Multiple studies have already been conducted in the literature on reduction of wind load through mirror face modification. Researchers have studied the effect of an increasing gap between heliostat facets has on the wind load [28]. This study was conducted both experimentally and numerically. The experimental heliostat was a polymethyl methacrylate 1:10 scale heliostat placed in a wind tunnel. The heliostat facets had variable gap sizes of 0–40 mm. The experimental study found that increasing the gap size did not significantly change the mean wind load coefficient. The numerical study found that increasing the gap size increases the wind load, but only slightly. The gap size did not have a significant enough effect on wind load to be considered in heliostat design for reducing structural requirements. However, this study also found pressure coefficients, lift coefficients, drag coefficients, and moment coefficients on a heliostat at different incidence angles of wind, data that are very useful in heliostat design.

Ahlbrink et al. [29] studied the wind loads on heliostats and compared the moments resulting from the wind load at various aspect ratios of the facet panel. It was determined that for the reliability of the foundation and pedestal, a higher aspect ratio is favorable. The moment on the base of the pedestal is significantly reduced when the aspect ratio is higher. The elevation drive, which is exposed to a high moment at the hinge of the heliostat, also benefits from a higher aspect ratio as this moment is reduced. However, a high aspect ratio of the panel is not advantageous for azimuth drives.

Engineering for both cost-reduction and optimized reflectivity may represent another significant gap in mirror design. A survey study by Pfahl in 2014 considered cost reduction methods for heliostats including using aluminum mirrors [30]. Aluminum mirrors would be light weight with good rigidity and handling, low breakage, and would be suitable for monocoque constructions. However, they would have reduced reflectivity and extra costs for protective coatings against abrasives. This article referenced a study by Magdaleno López et al., which looked at aluminum surface solar mirrors over a 12-year duration in Mexico City. The mirrors were exposed to aggressive weather and abrasive particles in the atmosphere yet only had a reflectance decrease of 3%. Two types of aluminum solar mirrors have been studied primarily, mirrors with integrated first and second surfaces and first surface compound mirrors. However, some studies have assessed as much as a 26% decrease in reflectance from comparisons of glass/silver and aluminum reflectors [31].

A cost reduction study conducted in 2007 by Kolb et al. [32] evaluated cost reduction techniques for heliostats. Two cost reduction methods for heliostat facets were proposed. The first cost reduction method considered the use of a large stretched membrane facet. This facet would be developed for integration into a pedestal-type heliostat with a surface area of up to 150 m^2. However, the analysis found that the stretched membrane-type heliostat may not decrease heliostat cost or increase LCOE, so the concept was removed from consideration. Another stretched membrane facet was considered that would replace welded stainless-steel strips of traditional heliostats with a single large fabric. The method would remove the need for expensive stainless-steel strips and expensive welding techniques as the fabric would be mounted using press-fit concentric hoops. The fabric would be impregnated with a sealer to avoid air leaks into the facet plenum environment. However, rough calculations in the study suggested that heliostat cost per square meter could be reduced by $7 with this method alone. In general, a cost reduction of mirrors/facets represents a significant gap. Current prices of overall heliostats are still nearly double the Department of Energy (DOE) SETO heliostat cost target of $50/m^2$. There are multiple pathways to cost reductions, including material selection, facet design, mirror gap, aspect ratio, and reduced design requirements through additional wind loading research. Soiling is known to reduce mirror performance over time, affecting O&M costs and ultimately LCOE. Antisoiling coatings provide the potential to maintain higher mirror performance at a lower cost, but standards are necessary to demonstrate both efficacy and durability of such coatings.

Additionally, a relatively recent study considered heliostat faces of size 8, 32, 64, 96, 120, and 148 m^2 for cost analysis [33]. The study considered the component costs for pedestal and truss structures, drives, mirror modules, drive control systems, field electronics, and design overhead for each size. Overall, 8 m^2 heliostats were the most expensive. Prices decreased at 32 m^2 and bottomed out at 64 m^2. From that size on, the price increased again. However, even at the considerably large size of 148 m^2, the cost never exceeded that of the 8 m^2 heliostat. The 8 m^2 was more costly in almost every category except for the pedestal and truss system, which predictably increased in cost for increasing size, and the mirror module cost which was the same for all sizes. The most expensive component for the 8 m^2 size was the drive.

The Google prototype heliostat explored the use of a custom reflector made entirely of glass to keep manufacturing costs down and to keep the system lightweight [34]. The system used a matrix of rectangular optical quality glass mirror sheets, mounted on a glass honeycomb back board. The honeycomb was constructed from segments of glass bonded to glass backboard on the back and the optical quality glass mirror on the front. The glass sheets were annealed glass instead of tempered glass, which kept costs low but reduced strength. The system was cheap and light weight and eliminated thermal expansion issues, all factors that translated to a cheaper frame and truss support system. The reflector was slightly curved to increase the concentration ratio. The system was designed to be lifted with vacuum lifters. A hail gun was used to fire an ice ball at the reflector to simulate 25 mm hail in accordance with IEC 61215A, which the reflector survived. However, the mirror was only tested via finite element analysis (FEA) in standard load conditions. High wind scenarios were not tested on this entirely glass reflector.

2.3 Torque Tubes. Torque tubes are an important component of T-type heliostats but do not vary significantly between heliostat designs. Traditional torque tubes in heliostat designs are constructed out of steel round tube or pipe. For a T-type heliostat design, a torque tube acts as a central horizontal rotational axis and is a key part of the facet support structure. The single axis can be used for rotation to vary elevation angles and mounting of welded truss systems for support of mirrors. Torque tubes also effect heliostat stow position. Mammar et al. [35] conducted computational fluid dynamics and wind tunnel studies on heliostats to evaluate the effect of wind speed on torque tube heliostats. It was found that the torque tube design has a significant effect on the choice of stow position that will result in minimized moments. With respect to most torque tubes, the optimum stow position cannot be perfectly horizontal at high wind speed. The inclusion of a torque tube was also shown to reduce the vertical force component in wind. Their results showed that vertical forces were reduced at all elevation angles between 0 and 90 deg with the use of a torque tube and computational fluid dynamics validation experiments. Torque tubes are large and heavy, which may unnecessarily contribute to the specific costs of a heliostat and the mass loads on the pedestal. They tend to be constant geometrical sections/profiles for convenience of cutting/welding with cantilevered loading, rather

than tapered to reduce material and costs. The mass and volume of materials used could be optimized while still maintaining adequate strength to prevent bending under high loads.

Some torque tube optimizations have been performed in the literature. In particular, Benammar and Tee [36] modeled heliostat components and analyzed the structural reliability at high wind speed. The torque tube was modeled considering gravity and wind as the main loads, which could cause deformation. The torque tube was modeled with the center of the tube jointed at the top of the pedestal, eliminating deformation at the center of the tube and maximizing points of bending deformation as the end points of the tube. The maximum wind load was applied to the center based on the accepted assumption in the literature that wind loads are centered on heliostats. Two torsion loads were considered, generated by wind and by mirror weight. Based on this model, it was determined that the torque tube element is a critical component that needs to be improved. Recommendations are that for small heliostats at sites with low wind speed, a thick torque tube with a small diameter is most reliable. However, at locations with high wind speed, a thin torque tube with a large diameter will be most reliable. It was also found that in the stow position, heliostat torque tubes can have the relatively low reliability, especially as compared to the pedestal and truss system, as wind speed increases.

In several recent applications, torque tubes have been eliminated entirely in several recent applications. At Atacama I (operational since 2021), the mirror facet support structure is entirely trussed. The Abengoa ASUP 40V3 heliostats used at Atacama I are shown in Fig. 3 [37]. Facets may also be suspended from a central pylon, rather than supported from underneath. Suspension-style solar trackers are being developed by Solaflect and Skysun LLC. Originally developed for heliostat applications in collaboration with National Renewable Energy Laboratory (NREL), suspension structures can reduce steel consumption by two-thirds relative to a standard pedestal design [38].

2.4 Pedestal. The pedestal is typically a vertical support, which like the torque tube, is often a large round, square, or rectangular steel tube. The pedestal is firmly secured to the ground with the use of anchors and a relatively large foundation. The use of large and rigid mechanical bodies is necessary for when a load is applied on the pedestal and the pedestal foundation during high wind conditions. As with torque tubes, the pedestal and foundation cost, strength, and weight are functions of raw material cost since these components are often made of concrete and standard steel components. However, these components can also be optimized for the most cost and weight efficient dimensions while maintaining high strength and bending resistance. Benammar and Tee [36] modeled heliostat components and analyzed the structural reliability at high wind speed. In their model, the total bending stresses on a pedestal were stated with respect to applied wind loads, mirror weight, and compressive stress [39]. Pedestal reliability was found to be lowest with mirrors in the vertical position and highest in the horizontal stow position. Maximum bending moments occur at the base of the pedestal. The study attempted to optimize the reliability of the pedestal given these bending moments and wind load conditions, using a round steel tube as the pedestal. The study increased the inner and outer diameter simultaneously or the wall thickness, but not both at the same time. It was shown that both increasing pedestal diameter and thickness increased the reliability in these models. However, increasing the thickness had a significantly greater impact. Increasing the pedestal diameter only had a small impact on reliability.

The pedestal foundation can also be optimized for strength or low cost. Pfahl et al. [40] have extensively studied heliostat cost reduction methods including the use of a prefabricated concrete ground anchor foundation. Traditional concrete foundations typically use rebar, steel anchors, and concrete to secure the pedestal to the ground. However, the authors noted that such foundations for heliostats typically contribute about 10% of the total heliostat cost. To reduce this cost, the authors considered a prefabricated concrete foundation block, which is built to accept natural material such as sand or rock. The material is removed from the foundation installation site and then placed back on the foundation, partially burying it in rock or sand. The addition of site material to the foundation block would decrease costs. It would also make transportation easier, as the pre-installed foundation would be lighter. Significant cost reduction is expected for this method. To improve soil characteristics, stabilization and exchange methods that are standard in coastal protection could be applied.

Pedestal foundations can also be eschewed with carousel-style rim drives. One such example is the Solar Dynamics SunRing, which accomplishes azimuthal rotation with a geared ring riding on ground anchors. Kurup et al. [26] showed that the foundation cost of $\$2.07/m^2$ is higher than that of a heliostat with a traditional single foundation. However, site labor costs were reduced by $\$8.60/m^2$, partially as a result of a semi-automated pile driving procedure replacing the laying of a standard foundation.

While the pedestal, like the torque tube, does not represent a significant gap outside optimizing the design for material usage and reliability, the pedestal foundation has more room for improvement. Numerous methods exist for fixing a large structure such as a heliostat to the ground, and an optimal methodology could be developed that allows for ease of transportation, optimization of material usage, and good rigidity and resistance to wind and mass loads.

Fig. 3 Abengoa trussed heliostat at Atacama I. This design eliminates torque tubes entirely. This can lower the structure's cost in two ways. First, less material (by mass) is used. Second, there is no need to separately procure and process a small quantity of one specific tube/pipe size for the torque tube. Adapted from Ref. [37].

2.5 Structure and Truss System Components. Nearly all commercial heliostats use a pedestal that supports a rotating torque tube [41]. These structures tend to be fabricated from structural steel and are therefore material intensive. The mass of steel in a heliostat structure can range from 59 kg/m^2 for a pedestal design to 15 kg/m^2 for an optimized spaceframe [42,43]. A large mass of raw material inputs into assemblies (e.g., steel into the heliostat's structure) is not only a significant cost but one that is inherently susceptible to large fluctuations in commodity prices.

Some variegated geometries that potentially reduce material usage are in commercial use. Heliostats manufactured by eSolar, in use at the agriculture firm Sundrop Farms' South Australia CSP facility since 2016 and pictured in Fig. 4, use a ballasted truss to support each heliostat, largely eliminating pedestals and concrete foundations in the process. Peterka and Derickson [44] provided progress for a heliostat development that comprised glass directly bonded to a formed sheet steel frame in use since 2011 in a research application. The Stellio heliostat, installed at the CEEC Hami 50-MW plant, reduces wind loads with a pentagonal shape and circumferential purlins supporting its facets.

Truss systems vary between heliostat designs such as large T-shaped heliostats with torque tubes or small heliostats with

Fig. 4 eSolar trussed and ballasted heliostat 24,000 mirror modules mounted on shared trusses are used at the SunDrop facility. The diminutive heliostat represents a design approach that focuses on minimizing cost of installation at the site; according to eSolar, installation used local unskilled labor, with only one size of wrench needed for complete assembly. Adapted from Ref. [3].

single U-joint connections. The truss system also involves bolts, welds, and adhesives that may be used as attachment and pinning methods. These attachment methods must take into account material rates of thermal expansion. Glass and steel mirrors use different pinning methods due to different facet weights and facet rates of thermal expansion. Facets are typically fixed with pins that allow flexing and rotation. These pins are mounted above the torque tube and must be capable of holding the weight of the facets. These pins are often mounted to the facets using glue and pads for increased surface area and to avoid damaging the facets. This is another potential gap area that could be improved and studied, though it is dependent on other components of a specific heliostat such as mirror design.

As with many components of heliostats, wind loads can impact the mechanical integrity of the truss system. The widespread availability of wind load data may better demonstrate what components of the heliostat structure are overbuilt and what components require reinforcement. For example, Emes et al. [19] have studied pedestal and hinge bending moments that occur in unsteady pressure distributions at a turbulent atmospheric boundary layer. Pressure distributions on heliostat faces can be nonuniform due to turbulence and can cause significant bending moments at the base of the pedestal and at the hinge. Their study found that at the hinge the bending moment is strongly correlated to the center of the pressure distribution and the movement of this center. It was also found that the bending moment at the hinge is highly correlated with turbulent energy. This study is significant as turbulence in heliostat fields can be high. As found by Peterka and Derickson [44] heliostats increase turbulent kinetic energy as wind flows through a field. Studies like this demonstrate turbulent movements of center of pressure distributions could significantly improve heliostat support structure engineering.

While extensive FEA is typically involved in the construction of a truss system, reliability analysis is needed. Benammar and Tee [36] modeled heliostat components and analyzed truss structural reliability at high wind speed. In their model of the heliostat truss system, a heliostat with four identical truss systems was considered. This is difficult to model for reliability since truss systems can vary greatly. However, useful reliability information was still gained.

Wind and mirror weight loads were considered as external forces were applied on the truss. The assumption was made that wind loads concentrated at the center of the heliostat as well as the center of the individual truss systems. In most models of the truss system, reliability did not change. However, it was noted that in one case where the cross-sectional area of the truss system was increased, reliability of the truss system across a range of wind speeds was improved.

Many alternate support systems have also been designed that differ from traditional truss systems built around a vertical pedestal and horizontal torque tube. The Google prototype heliostat developed in 2010–2011 [45] used a simplified tripod truss system to mount the entire heliostat. The system had a single large beam at the front making a 90 deg angle with the ground, supported by two 45 deg cross members running from the top of the vertical beam to the ground. Horizontal beams were mounted in between these members for additionally rigidity and support. The system used ground anchors which would run through holes in the frame and screw into the ground. The specific frame was designed to be small, lightweight, and even foldable for easy shipping and delivery to a target plant site. The specific frame was built for a 6 m^2 heliostat panel and contributed just \$11.70 to the \$/m^2 cost of their heliostat, though the design could easily be scaled up for larger heliostats. The frame was made of galvanized steel C-channels and was riveted together instead of welded.

Space frames have effectively reduced material usage (and therefore cost) in noncommercial applications. A prototype space frame design documented by Davila-Peralta et al. [42] reduced steel usage to 15 kg/m^2, a mass elimination of two-thirds from a conventional T-type heliostat. The use of space frames, however, typically also necessitates the use of rim drives or other actuation methods.

Trusses can be avoided entirely with a membrane-type mirror panel approach. This suspends the entire mirror surface from a central pylon using cables, using the mirrors themselves as structural members in compression. Coventry et al. [46] note that this can reduce overall material usage by 60–65%. In heliostat applications, Solaflect's William Bender calculated a \$25/m^2 reduction in installed cost for the suspension heliostat, of which nearly two-thirds stemmed from reduced material usage [47]. Solar-tracking PV arrays, manufactured by Solaflect Energy, are commercially available using this style of construction and actuation.

3 Controls

Heliostat control systems ensure that each individual heliostat in a field tracks the angle bisector between the sun and the solar receiver [48]. Control systems also manage the incident irradiance on the receiver by varying the number of heliostats in use. For every CSP system, the number of heliostats pointed at the receiver needs to be adjusted depending on the sun's position in the sky. For example, at noon in the middle of summer, fewer heliostats need to be pointed at the receiver than late in the afternoon on a winter's day.

Control of each individual heliostat may be open- or closed-loop. As elaborated by Sattler et al. [48], this is not a binary distinction. Fully closed-loop systems possess a beam characterization system, which provides feedback data based on where each heliostat's beam hits the receiver. Some approaches to closed-loop controls can enable automatic rough calibration as part of commissioning and fine calibration on a daily or even more frequent basis. Full closed-loop control requires sensing of all heliostats while they are simultaneously tracking to a receiver. A white Lambertian target can be used for some off-target closed-loop control during calibration, however in some cases, heliostats can then return to open-loop control once they are on the receiver. A goal of closed-loop controls employment is to decrease commissioning and O&M cost and increase long-term plant performance. For

example, the National Renewable Energy Centre of Spain demonstrated that 0.6 mrad directed beam direction error is achievable with heliostats using consumer-grade 5-megapixel CMOS cameras for calibration [49]. Some form of closed-loop control is implemented in heliostats from Abengoa, BrightSource, and Supcon (Cosin) Solar, comprising the majority of central receiver facilities that have been online since 2013. The hardware to enable closed-loop heliostat control is also capable of providing feedback for plant-level control. At Ashalim, for instance, the PV panel mounted to each BrightSource heliostat provides irradiance data back to field management software. This software is able to therefore decide, in real time, which heliostats to aim at the central receiver to maximize flux in, for instance, partially cloudy scenarios [50].

Partially closed-loop systems use measurements beyond data from the heliostat's drive encoders – tracker-mounted cameras, for instance. By using specific definitions, Sattler et al. identify 30 unique closed-loop calibration schemes as the current state-of-the-art, sorted into five classes [48].

Simple illustrations, as shown in Fig. 5, help to explain the five different classes (A1, A2, B, C, and D) of techniques that have been explored for closed-loop calibration systems.

When a heliostat's reflected light spot is pointed toward the target, control of the heliostat must transition from rough aiming to precise, on-target position control. This can be facilitated using mounted accelerometers that can capture relative position and motion data. There are two important components of this transition: capture strategy and capture detection. "Capture strategy" is lining up the heliostat angle with the target so that on-target position control can sense it and "capture" it. The heliostat accelerometer has an accuracy of a degree, while the on-target position control has a tighter resolution of 5 mrad (about 0.25 deg). Because of these differences, it's possible that the heliostat could think it's pointed directly at the target, while the target is unable to see it. The accuracy of accelerometers should be sufficient most of the time to capture position data. If it misses, the heliostat could move in a spiral pattern – tight, widening circles – until the light spot is captured.

Capture detection happens when the on-target positioning system detects the location of a light spot from a specific heliostat in its field of view. At this point, the heliostat's control system switches from relying solely on the accelerometer to relying on the on-target spot position sensing system, which has far higher precision and accuracy. When a heliostat field tracks the bisector and directs sunlight, tracking error can occur. As described by Sattler et al. in their review article, heliostat tracking error has very low tolerance and is usually measured in units of milliradians, equivalent to 0.057 deg [48]. An example of this tolerance is given with a heliostat 1 km away from a target, where a 1 mrad tracking error would put a beam 2 m away from the desired aim point. Tracking errors can source from gravity bending, gear ratios and backlash, pivot point offset, dust refraction, angular offset, leveling and other installation errors in the heliostat, poor installation of the torque tube relative to the pedestal, poor heliostat design relative to wind and mass loads, low encoder resolution, and even disagreements between unit systems used by different engineering groups [51–53]. Of these errors, gear ratios, backlash, and encoder resolution are some of the major contributors [54]. Tracking errors alone represent a significant gap in heliostat design, as errors above 1 mrad can easily account for 10–20% losses in expected energy collection [55]. Montecchi et al. [56] monitored heliostat beam quality, mirror module performance, durability, and tracking accuracy in the wind from 1986 to 1992 at Sandia National Labs and compared ATS and SPECO heliostats. In winds ranging from 11 to 27 mph, the ATS heliostat had a maximum beam deviation of 3.7 mrad, average deviations of 0.92 mrad, and average maximum beam

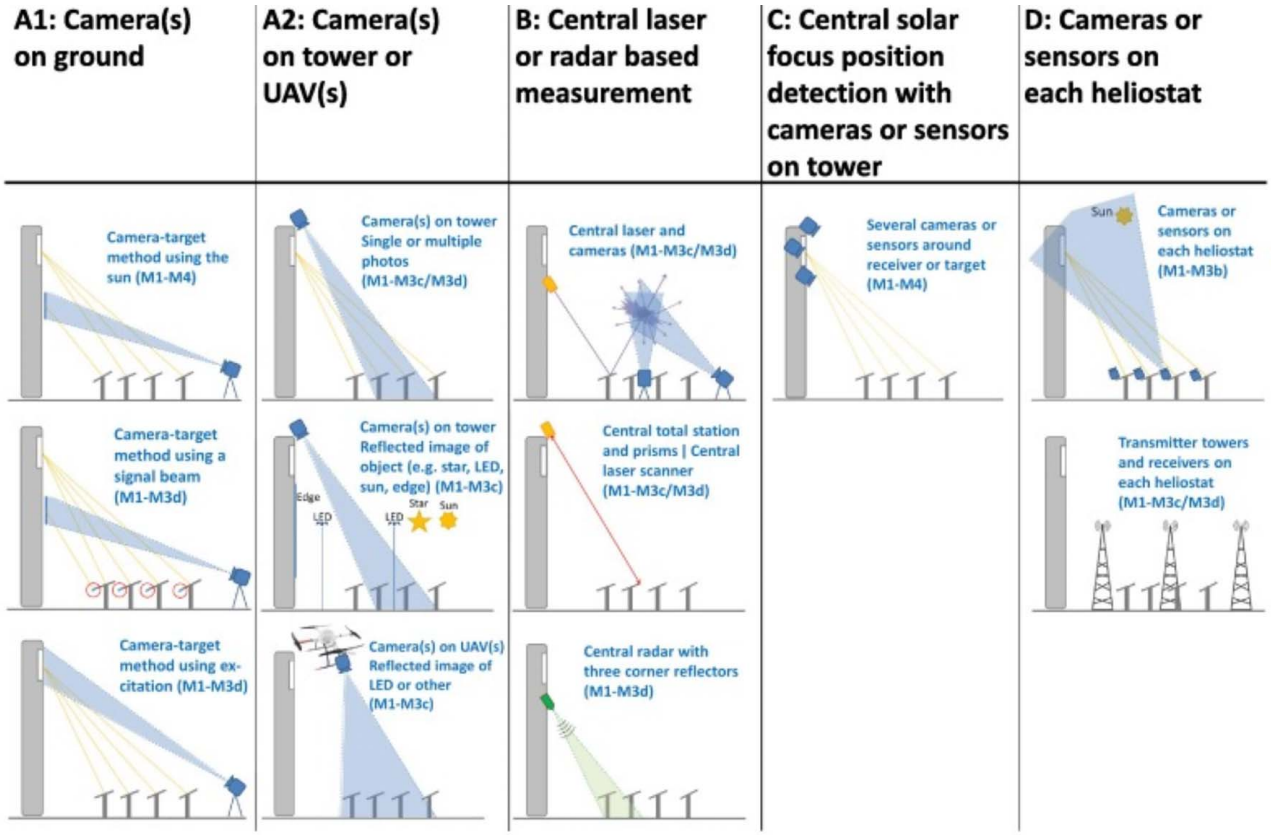

Fig. 5 Five classification schemes for automatic calibration of heliostats demonstrate that methodologies vary, and there is currently no broadly accepted strategy for closed-loop calibration and control. Adapted from Ref. [49].

centroid deviations for all observations of 1.9 mrad. The SPECO heliostat had a maximum beam deviation of 4.7 mrad, average deviations of 0.86 mrad, and average maximum beam centroid deviations for all observations of 1.9 mrad. The study found that overall, for the course of 6 years of observation, both heliostats were structurally rigid enough to perform within their design specifications in real-world wind scenarios.

To account for tracking errors and maintain accuracy in a heliostat field, further control systems must be in place. Many heliostat systems use open-loop tracking to accomplish these goals. They stay on target by following a preset course given their known positions in the field and the known course of the sun in the sky. This requires heliostats to be placed precisely on level graded land on a firm foundation. Other control systems are closed-loop, measuring and recalibrating the field based on input data every few seconds.

Traditionally, many heliostat field systems employ open-loop controls tracking (which does not require sunlight to operate), where heliostats stay on a receiver target by following a preset trajectory based on their known positions within a respective field layout, the time of year/day, and based on their geographical location. For closed-loop heliostat control, coarse and fine motion refinements are accomplished using sensors located on the heliostat as well as those on the receiver (Fig. 6). Communication between the two sets of sensors through the field computer and individual heliostat computers allow for course orientation control. Here, multi-axis accelerometers as well as employment of a precise, target-mounted light spot position sensor can be used for alignment within few degrees of accuracy [48]. Additionally, on-target position control using a photometry system to position light spots around a target calibration panel or receiver can be used more fine refinements. Depending on the receiver geometry, pointing accuracy would need to be sufficient to allow precise control of the heat distribution [48].

For closed-loop control systems, generally the goal is three-fold:

- Rough orientation control of the heliostat using a reflector-mounted three-axis accelerometer for alignment within few degrees of accuracy.
- Capture of the heliostat's light spot by a precise, target-mounted light spot position sensor – in our case, a multi-scopic photometry system.
- Precise, on-target position control using a photometry system to position light spots around a target calibration panel or receiver. The pointing accuracy would need to be sufficient to allow some control overheat distribution across a specific target such as a heat exchanger in a receiver down to 10–50 cm resolution [57].

During operation when a heliostat's reflected light is pointed toward a receiver, control of the heliostat must transition from coarse to fine resolution refinement, which requires both on-board sensors (e.g., accelerometers) as well as on-target or receiver position control. To make the transition seamless, one must consider the capture strategy and capture detection. The capture strategy is lining up the heliostat angle with the target so the receiver spot position control can sense it [58]. Capture detection occurs when the on-target positioning system detects the location of a light spot from a specific heliostat in its field of view. At this point, the heliostat's control system switches from relying solely on heliostat sensors to relying on receiver spot position sensing system or photometrics, which can have a significantly higher precision and accuracy [58].

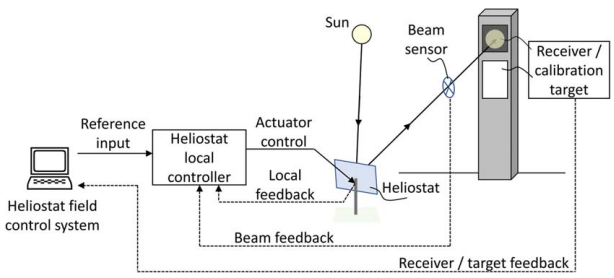

Fig. 6 Closed-loop heliostat control configuration example [49]

Closed- and open-loop control systems must be five to ten times more accurate than the desired tracking error, meaning 1 mrad tracking error requires 0.1 mrad error in the control system [58]. This requirement alone represents a significant gap in the heliostat design. However, important distinctions must be made between closed-loops and open-loops in heliostat control, as the distinction is not always clear, and there is a significant overlap. Examples and definitions are provided in Sattler et al. [59], Malan et al. [60], and Swart [61] for open and closed heliostat control loops. Given examples state that a typical signal or effect in a control loop may flow through components starting from the control room to the controller, then to an actuator, an encoder, a sensor on the heliostat, mirror and surface normal influencers such as drives, to the target. Measuring devices in this loop may include computers, encoders, sensors, cameras, beam characterization systems, and other devices for measuring heliostat and mirror normal. Closed-loops will use the measuring devices for feedback to input into the loop of the signal and effects. Heliostat closed-loop systems will typically use the beam characterization system for feedback to input into the control system. However, partially closed-loops also exist, which use feedback from individual heliostat and mirror normal measuring devices as input into the control loop [60]. Even open-loops are not always pure open-loop systems, as closed-loops will still exist between the control room, drives, and encoders.

Many heliostat control systems will stop at this point without verification that the beam has reached the target [62]. Some have integrated a closed-loop component by adding a beam characterization system, which can be used for simple verification by the operators or can actually close the loop with feedback.

Open-loop control systems for heliostats represent a significant gap that could be improved. Adding measurement devices for flux at the receiver, spillage, aiming errors, with feedback, could significantly reduce tracking error. While open-loop tracking has errors up to 1–2 mrad, closed-loop tracking systems with simple measurement devices can easily reduce error to 0.1 mrad [54]. Though more error can still be accounted for, such as shifting foundations or warpage from wind, devices that can measure heliostat parameters such as perpendicularity of the torque tube relative to the pedestal or foundation level could be integrated. Along with heliostat pointing vector measurements or even mirror normal vector measurements, control loops could be further improved.

For a deployed CSP system, heliostat receiver pointing requires timely and accurate adjustment depending on the sun's position in the sky. A field controls management algorithm is employed to actively determine which specific heliostats should be pointed at a given receiver, as well as which should be held in reserve. Heliostat field control systems are designed to direct sunlight at a specific target within 1–2 mrad accuracy [63]. Controls algorithms, along with heliostat operators, leverage feedback from a heliostat computer to track the sun movement; however, adjustments over time are required for simultaneously correcting externalities such as wind, foundation shifting, and thermal expansion. In addition, control systems employ tools such as a beam characterization system to monitor and adjust the amount of thermal power reaching a receiver to a predetermined thermal envelope. Here, control systems are designed with dynamic optimization algorithms to operate within the integrated CSP system at the most profitable points of power generation depending on the time of day and year.

While the potential cost and performance benefits of closed-loop control are obvious, Fig. 5 demonstrates that the industry has not come to a consensus on a best technique. The differing options are not well understood for variation in cost, difficulties in implementation, limitations in optical accuracy, and long-term field performance and required maintenance. In order to achieve bankable benefits of closed-loop control and calibration, more research and

Fig. 7 Wireless BrightSource heliostat at Ashalim with top-mounted PV panel. A small heliostat is estimated to consume less than 1 kWh per day [69]. Heliostat-attached PV panels can therefore provide feedback data and eliminate power cabling. Adapted from Ref. [51].

development is needed to come to a consensus on the most beneficial implementation techniques.

3.1 Wireless Controls. A truly wireless heliostat is not only controlled but also powered, wirelessly. Traditionally, heliostats have been controlled by buried copper or fiber optic wired networks, but in recent years, there has been movement toward wireless communications. Wireless communications offer simplified plant design and cost reduction due to both material reduction and reduced labor hours at construction. In the heliostat space, Solar Dynamics, Trinamic, BrightSource, and others have introduced wireless heliostats. At Ashalim (operational since 2019), BrightSource equips each wireless heliostat with a PV panel (Fig. 7). The need for cabling is thereby reduced by 85% or more [20]. The PV panel provides not only power but also heliostat level irradiance data – feedback that enables field management software to fine-tune receiver flux [19]. Glatzmaier et al. [64] assessed the cost and performance benefits of a wireless system for heliostat power and control. Through an extensive survey, analysis, and model development, his project quantified and compared the cost of their shared-node wireless system to be 42% less than the cost of a fully wired system that is representative of the state-of-the-art technology for commercial power tower plants [67].

Heliostat fields present an opportunity for deployment of low-power wide area networks, which are already heavily utilized for Internet-of-things solutions. PV tracker systems have in recent years operated with wireless communications, where lessons learned can be utilized for CSP heliostats. For example, Nextracker (a single-axis PV tracker company) was founded in 2013 and begin installing utility-scale PV plants with solar trackers controlled by Zigbee wireless communications and small PV panels and batteries for power. Nextracker now has over 50 GW of installed trackers operation on Zigbee wireless networks [65]. While single-axis trackers are simpler to control than two-axis heliostats, such installations have proven the possibility of cost reduction using wireless control.

Although wireless systems offer cost reductions, various approaches could introduce significant technical, cybersecurity, and other safety issues. There are currently no standardized requirements and testing capabilities to validate both functionality and safety as the CSP industry transitions to fully wireless control.

3.2 Component Integration. Component integration and overall heliostat field design represents another gap. Improvements in modeling capabilities have allowed for extensive computational fluid dynamics wind modeling and optimization modeling that could be used to significantly improve heliostat field design and component integration. In 2018, Wang and Pye [30] developed a high-dimensional genetic algorithm toolbox for optimizing entire heliostat fields. The toolbox was used to optimize the Gemasolar plant. The toolbox was used to optimize multiple factors at once by row. The spacing between the tower and the first row of heliostats was optimized, the distance between one row and the subsequent row, the spacing of heliostats in the row, and the height of pedestals in a given row were all optimized. The article showed that the model could be used with great success for optimizing a specific power tower plant. In the example case given in the article of optimizing the Gemasolar plant, the optical efficiency could be increased to almost 64% and the annual insolation weighted efficiency could be increased to 57%.

Alternate heliostat integration systems have also been described in the literature [66], such as ganged heliostat systems which have also been optimized with facet torque tubes within the overall heliostat system [67]. The torque tube heliostat system [68] has all facets mounted on single torque tubes that are coupled in rows. When the coupled torque tubes are rotated, the facets in a single row all have the same elevation angle. The system was modeled with a simulated 210 MW_{th} tower plant with a 12-m by 14-m receiver. The heliostat field had a reflective area of 120 m^2, modeled with the heliostat field tool HFLCal. The distance between rows of torque tubes, the distance between the first row and the tower, and the facet distances were all optimized. The weight of the system was also optimized. The system would potentially be far cheaper to build and install, with a simpler control system, and only had a 3% yield reduction when modeled against a traditional tower and heliostat field of the same size and output.

Extensive wind tunnel and computational fluid dynamics wind modeling have increased the available information for heliostat field design significantly [69]. Reactions of both individual heliostats and heliostat fields are better understood, and designs could be improved with this information. Research by Emes et al. [19] on pressure distributions across heliostats also looked at design wind speeds. The article did conclude that, based on peak hinge moments, maximum design wind speeds could be increased for a 36 m^2 heliostat. The hinge moment data showed that wind speeds of 29 m/s in a desert, 33 m/s in a suburban terrain, and 40 m/s at stow were all possible for a heliostat with proper drives. However, operating loads decreased by up to 70% for the same conditions when the elevation angle was greater than 45 deg. The overturning moment occurring at the base of the pedestal was also determined, and to stay below the overturning load at angles elevation angles less than 45 deg, design wind speeds would be 18 m/s for a desert and 21 m/s in a suburban terrain.

3.3 Concentrating Solar Power Heliostat Components and Controls Industry Survey and Gaps. To identify and determine the most challenging gaps that impact the cost, performance, and reliability of heliostat component and controls systems, this investigation facilitated a survey that was circulated to CSP heliostat designers, plant operators, and those involved in bankability. The survey questions were the following:

- What are the top problems you have encountered with heliostat components and controls during the installation and commissioning phase of CSP plants?
- What are the top reasons for heliostat downtime in the operational phase of CSP plants?
- What are the most expensive repairs (including labor hours) for heliostat O&M?
- What are the most unreliable components for heliostats (including controller components)?
- What are the most significant challenges in maintaining heliostat performance, including desired targeting alignment?
- Have you had significant issues with soiling and cleaning of heliostat mirrors? If so, please describe the issues and the cleaning methods used.
- Do you see a direct need for codes or standards to improving commissioning or operations of CSP plants? If so, please list specific areas you see the need for codes or standards.

Table 1 Tier 1 gap analysis for components and controls

Tier 1 gaps	Functionality of solution	Justification/benefits	Recommended pathway
C1 Lack of lightweight composites or other advanced structures (e.g., torque tubes, pedestals, foundation) are necessary for hitting cost targets.	Lighter-weight construction; increased reliability and lifetime; lower costs of fabrication, transportation, and deployment	Steel and foundations cost ~$\$24/m^2$ per 2020 in the most recent NREL cost analysis. Steel costs jumped 200% in 2021, demonstrating the high sensitivity to this commodity cost. These numbers demonstrate the need for drastic change if $\$50/m^2$ is going to be achieved.	Funding to research initiatives focused on alternate materials and structural designs outside the typical pedestal heliostat design. Funding to support testbeds for examining alternate designs coming from industry. Publication of a proven heliostat design qualification standard that would provide industry the necessary tool for validation of new designs outside the status quo.
C2: Lack of lower cost mirror designs with comparable performance to existing glass mirrors.	Mirror facets are designed for optimal performance and manufactured at volume to achieve cost reduction.	Mirrors and their supports cost $\$24/m^2$ per 2020 commercial heliostats. This would account for nearly 50% of a $\$50/m^2$ target and therefore does not leave sufficient dollars for the remainder of the heliostat.	Funding provided to research and develop composite/sandwich or other mirror designs that can achieve cost reductions.
C3: Wireless systems approaches are needed to capitalize on lower plant cost, while wireless risks and technical issues must be avoided. Standardized requirements and testing capabilities are needed.	IEC standards are published that enable the safe and effective use of wireless controls.	Robust signal communication R&D needed for resilient wireless controls. R&D needed for wireless advanced controls architectures and hardware for facilitating single node or mesh networking.	Develop wireless testbeds to characterize signal abatement/loss and networking architectures. OR Adapt current wireless testbeds for heliostat field operations, size, and configurable topologies.
C4: Lack of closed-loop systems that are applied to achieve higher flux performance and auto alignment/calibration processes.	Closed-loop controls and various feedback sensors are a well understood, bankable solution to automated calibration, reduced drive requirements, and maintaining long-term heliostat performance.	More robust closed-loop communication needed for all operations within a heliostat field, such as with calibration and general commissioning.	Closed-loop communication R&D funding and testbeds for evaluating novel sensors and controls architectures. This includes R&D to address automation for calibration and commissioning as well as costs, while reducing field error.
C5: Missing design qualification standards for heliostats to enable bankable components and controls, heliostat long-term performance, and shorten design improvement cycles.	IEC design qualification standards are validated and published. Any new heliostat design is subjected to this standard to prove market entry.	Bankable design qualification standards allow for rapid feedback on new designs that target cost reductions. This feedback enables further improvements in design and a real pathway to achieve $\$50/m^2$ cost targets. Without such standards a new design may never be given a chance or may be installed in the field and failures are found after millions of dollars of expenditures.	IEC 62817 is a design qualification standard for solar trackers and was intended to also cover heliostats. At the time of writing, there was not sufficient support from the heliostat industry to include several key sections related to heliostats. It is a low-hanging fruit to develop 62817-X, which includes the additional language specific to heliostats. This approach will take advantage on a number of appropriate existing tests as well as shorten the development process.

Table 2 Tier 2 gap analysis for components and controls

Gaps – Tier 2	Functionality of solution	Justification/benefits	Addressing strategy
C6: Alternatives are needed to impact design being driven by worse case wind loads as this is a significant boundary to cost reduction.	Lower torque drives can be used Variable drive sizing between inner and outer field locations Wind fences or other field modifications to minimize wind loading.	Cost reduction in drives and heliostat structure can be achieved with more detailed wind data or field design to reduce forces due to wind.	Funding provided to wind research specifically to the problems indicated for CSP.
C7: Alternate drives for cost reduction have not been fully explored.	Alternative drives such tip-trackers with two linear actuators are installed at scale and achieve bankability.	In the most recent NREL, cost analysis drives cost \$28/m^2, and this must be reduced to achieve \$50/m^2 for the entire heliostat cost.	Funding for better wind data per C6 opens opportunity for different drives, publication of proven heliostat design qualification standard enables bankable testing of alternate drives, or funding directly to drive development or drive test beds.
C8: Coatings for mirrors needed to improve performance and reliability.	Durable antisoiling coatings are applied to mirrors and result in less cleaning and higher effective reflectivity.	Mirrors must maintain high reflectivity and reliability for 30 years.	Funding provided to develop advanced coatings. Utilization of coatings formulations and R&D best practices from PV industry.
C9: Mirror quality should be adaptable to environmental conditions, but there are no standards for this.	Environmental testing standards are linked to degradation-based climate zones. Optimization is achieved by pairing mirror design to installation environment.	CSP plants are being installed in differing environments and mirrors are being overdesigned to handle all these environments. This means that cost reduction is left on the table for some sites.	DOE funding past work to gather mirror performance and degradation data in various locations. These data were assembled in a database for further analysis to help determine environment specific accelerated testing for various environments. The database was never used due to funding cuts and therefore is a low-hanging fruit.
C10: Need performance standards for heliostats.	IEC heliostat performance standards published, and heliostats are tested to these standards through design phases, commissioning, and as needed throughout a plant's life cycle.	Without clear performance tests for heliostats systems can end up underperforming in the field and drive up the cost of electricity for CSP systems.	IEC 62817-X as mentioned in C5 offers an efficient way to take advantage of an existing standard while including the necessary performance testing. SolarPACES has already written some language around performance testing that could be included in 62817-X
C11: Need for CSP-centric durability standards for the glass and mirror.	IEC durability standards, including pass fail criterial, are published for CSP mirrors. The standards are applied to new mirror designs, coatings, and in manufacturing quality assurance.	Materials differences for various heliostat mirrors needs to be evaluated for developing more robust and accurate designs.	Research studies and tools needed for evaluating construction materials and reflective surfaces both from performance and reliability. Evaluation of best practices, test beds, and trade studies needed from other industries to further develop current mirror durability and performance evaluation capabilities.
C12: Design and O&M are not well coupled (especially problematic with drives/mirrors).	O&M is planned within a heliostat design enabling cost and financing models to include maintenance costs/ reserves necessary to achieve modeled plant performance.	When design and O&M are not well-coupled systems typically degrade faster than intended and underperform expectations (resulting in higher LCOE). By coupling these variables system performance can be upheld over the life of the plant, reducing LCOE.	Development of a heliostat design qualification standard (including testbed development where necessary) and reliability standards for mirrors is the first necessary piece to connecting design and O&M. The data/results from such standards help inform how a system will degrade per accelerated lifetime testing. Mean time between failures and other reliability data must be gathered on key components.
C13: Reliability/degradation/aging not well defined yet this can impact pointing accuracies and system performance over time.	Reliability/degradation of various components and controls are well understood. Designs to reduce cost include reliability/degradation trade-offs, and therefore, new designs are optimized for lowest LCOE over the life of a plant.	Without reliability/degradation models for components and controls, CSP system O&M is not appropriately planned. System downtime and system underperformance are the likely outcomes.	Data must be collected and made readily available for degradation of components and controls as well as mean time between failures for various components. Funding appropriate test beds as well as design qualification standards will help to generate necessary data.

Table 3 Tier 3 gap analysis for components and controls

Gaps – Tier 3	Functionality of solution	Justification/Benefits	Addressing strategy
C14: Flexible wired communication and controls interconnections needed.	Confident controls communications through a CSP field for varying operational modes. Ability to modify heliostat set configurations without signal transmission interruptions/attenuation concerns.	Robust communication hardware needed to ensure reliable signal quality between heliostat and field computer.	Reliability research of current interconnection hardware with respect to signal distribution under varying controls scenarios. OR Utilization of best practices for large-wired controlled systems from other industries.
C15: Heliostats are automatic mechanisms that can exert dangerous forces and create fire hazards.	Safety standards are published for heliostats and pass/fail testing to the standards is conducted on individual heliostats and heliostat plants.	Controls signals to heliostats will cause a heliostat to move, regardless of if there are objects or personnel in the proximate vicinity. Additionally, unintended movement could facilitate hazards including fire.	Engineering controls safety criteria, feedback, and hardware needed for addressing design and operations to ensure reliable movements that do not cause injury or damage.
C16: Safety is especially important for wireless systems. Redundancies within the controls will be critical especially for SCRAM operations.	Safety standards are published for heliostat wireless controls.	Signal loss or abatement within wireless systems could facilitate hazards, particularly for automated systems. Safety redundancies and immediate feedback needed within controls to guard against unintended movements or consequences.	R&D funding for assessing feedback architectures with a variety of sensors and wireless controls software/hardware. Research for leveraging resilient safety engineering controls to operate reliably during contingencies and SCRAM operations.
C17: Concerns over cybersecurity attacks on a heliostat field could create a variety of high consequence events.	Heliostat specific cybersecurity standards are implemented.	Detrimental impacts of hacking of controls systems could pose issues related to plant power production or hazards from unintended heliostat motion.	Funding for R&D to address cybersecurity within the field and single-heliostat level controls for guarding against unintended control. Administrative controls development to also provided additional safeguards.

- Is Heliostat resiliency and security a concern?
- Describe other issues or concerns regarding heliostats. (This question elicited a variety of responses with no overlap between respondents.)
- With respect to cost, reliability, and operability of heliostat components (and their control systems), what are the most important areas of R&D?

Through this literature review of the state of the art and the industry survey, technical gaps in components and controls for heliostat technologies were developed as summarized in Tables 1–3, which outline the Tier 1, 2, and 3 gaps respectively.

The results of the survey found that the primary problems affecting heliostat field operation. Calibration and alignment were the most common answers to all questions concerning the causes of heliostat downtime. Drives were the most commonly flagged components for unreliability and high cost of replacement. When it came to ongoing operational challenges, three categories received the bulk of responses: calibration, soiling, and pointing errors. Issues with pointing error in the field underscore the concept that meeting SunShot objectives with cheaper drives, structures, and mirrors cannot occur at the expense of performance.

The industry survey exposed a need to address design and fabrication standards for heliostats, with 85% of respondents agreeing that heliostat-specific standards are necessary. Specific requests for standards spanned the heliostat life cycle from design (wind loads) to deployed fields (site acceptance testing), reflecting the relatively custom and ad hoc nature of current field implementation. A larger proportion, 88%, had experienced issues with soiling. While soiling is traditionally considered an O&M domain, coatings can play an important role in mitigating soiling's LCOE burden throughout a plant's lifetime.

4 Conclusions

A literature review was performed pertaining to state-of-the-art heliostat components and controls. This review was intended to provide a comprehensive assessment of various technologies that comprise the structure and dynamic subsystems in a heliostat, as well as for the controls and communications. This work includes the results of an industry survey, in addition to the results of the review, to determine the primary gaps that can have the largest technical and cost impacts for heliostat systems. The results of the comprehensive gap analysis indicated that existing heliostat structural and foundation costs must be reduced to achieve the DOE/SETO cost target of $\$50/m^2$. Per current designs, steel is a large portion of heliostat cost, and therefore cost targets are very sensitive to steel price variation. Large, heavy steel beams are used for the construction of pedestals and torque tubes. Alternate designs are needed that either use less steel or use alternative materials that are lower cost. In addition, alternate designs that are better optimized can be achieved in conjunction with the closing of gaps surrounding wind loading (for example, the need for high-frequency wind data, understanding of wind loads throughout the heliostat field, or wind-mitigating designs). Additionally, wireless system approaches can reduce up-front capital expenditure through reduced wire and conduit use as well as labor reductions per elimination of trenching and wire pulling/assembly. Cost savings are only achieved if wireless systems do not create new modes of failure or safety issues. Development/demonstration of wireless control architecture, signal communication, and methods of hardware integration are needed for industrial-scale heliostat applications. Wireless technical and resiliency issues, tracking error, ease of integration, safety during a potential signal drop, ease of operation, and cybersecurity issues are all of concern.

Additionally, older heliostat field designs use variations of open-loop controls [70], and such systems require countless hours in calibration in the commissioning process and throughout the life of the plant as heliostats require O&M. The slow calibration process surrounding O&M reduces plant availability and overall

energy production. Open-loop control provides no mechanism to compensate for the degradation of heliostat drives, and therefore, drives must be overdesigned to compensate or optical performance will degrade with time. Alternatively, researchers and industry players claim the ability to use closed-loop controls for automated calibration, reduction of commissioning time and O&M hours, reduction of drive requirements, and overall cost reduction. Existing research and plant hardware demonstrate a direction for closing the gap of broadly applied closed-loop control, while proprietary motivations slow the process. There must be further research, development, validation, and publication of closed-loop methods that can be supported through a synergistic closing of key metrology gaps.

Finally, mature industries have standards that serve as a backbone for producing safe, reliable, high-quality products. Standards allow new features, cost reductions, or other design iterations to be seamlessly introduced without quality problems. A qualification standard for heliostat design, covering individual components and overall integration and performance, would improve project bankability, reduce commissioning time, enhance performance, and allow lower cost designs to more rapidly move from R&D to the field. IEC 62817 (design qualification for solar trackers) contains most of the necessary tests but needs certain amendments to be fully applicable to heliostats. Specific needs are a procedure for measuring performance accuracy of heliostats and specific tests for wireless controllers.

Acknowledgment

This article contains excerpts from chapters of the *Roadmap to Advance Heliostat Technologies for Concentrating Solar-Thermal Power*, published in September 2022 by the Heliostat Consortium, funded by the U.S. Department of Energy [1], as well as a SolarPACES 2022 proceedings paper written by the authors which is currently in production [2]. The full *Roadmap* report is available.[2] Sandia National Laboratories is a multimission laboratory managed and operated by National Technology and Engineering Solutions of Sandia, LLC., a wholly owned subsidiary of Honeywell International, Inc., for the U.S. Department of Energy's National Nuclear Security Administration under contract DE-NA0003525. Funding was provided by U.S. Department of Energy Office of Energy Efficiency and Renewable Energy Solar Energy Technologies Office. The views expressed in the article do not necessarily represent the views of the DOE or the U.S. Government.

Funding Data

- The US Department of Energy (DOE) Solar Energy Technologies Program (Award No. 38896).

Conflict of Interest

There are no conflicts of interest.

References

[1] Relloso, S., and Gutiérrez, Y., 2017, "SENER Molten Salt Tower Technology. Ouarzazate NOOR III Case," AIP Conf. Proc., **1850**(1), p. 030041.
[2] Coventry, J., and Pye, J., 2014, "Heliostat Cost Reduction—Where to Now?" Energy Procedia, **49**(1), pp. 60–70.
[3] Schell, S., 2011, "Design and Evaluation of Esolar's Heliostat Fields," Sol. Energy, **85**(4), pp. 614–619.
[4] Abengoa Corp., 2009, "Abengoa Solar Annual Report," Volume 1, Abengoa Corp, https://www.abengoa.com/web/en/accionistas_y_gobierno_corporativo/informes_anuales/2009/
[5] Koretz, B., 2014, "Flexible Assembly Solar Technology," NREL Concentrating Solar Power Program Review," NREL, https://www.energy.gov/sites/prod/files/2014/01/f7/csp_review_meeting_042313_koretz.pdf
[6] Gould, W., 2011, "SolarReserve's 565 MWt Molten Salt Power Towers," 16th SolarPACES, Granada, Spain.
[7] Lata, J., Alcalde, S., Fernández, D., and Lekube, X., 2010, "First Surrounding Field of Heliostats in the World for Commercial Solar Power Plants—GEMASOLAR," 16th SolarPACES, Perpignan, France.
[8] Kolb, G. J., Jones, S. A., Donnelly, M. W., Gorman, D., Thomas, R., Davenport, R., and Lumia, R., 2007, "Heliostat Cost Reduction Study," SAND2007-3293, 912923, Sandia National Laboratories.
[9] Benyakhlef, S., Al Mers, A., Merroun, O., Bouatem, A., Boutammachte, N., El Alj, S., Ajdad, H., Erregueragui, Z., and Zemmouri, E., 2016, "Impact of Heliostat Curvature on Optical Performance of Linear Fresnel Solar Concentrators," Renewable Energy, **89**(1), pp. 463–474.
[10] Mancini, T. R., Gary, J. A., Kolb, G. J., and Ho, C. K., 2011, "Power Tower Technology Roadmap and Cost Reduction Plan," Sandia National Laboratories (SNL), Report No. SAND2011-2419.
[11] IEC, 2014, "Photovoltaic Systems-Design Qualifications of Solar Trackers," IEC International Standard, https://webstore.iec.ch/publication/7442
[12] Nieffer, D., Effertz, T., Macke, A., Röger, M., Weinrebe, G., and Ulmer, S., 2019, "Heliostat Testing According to SolarPACES Task III Guideline," AIP Conf. Proc., **2126**(1), p. 030039.
[13] Röger, M., Kämpgen, A., Happich, C., Villasante, C., Nieffer, D., Guillot, E., Weinrebe, G., et al., 2023, "SolarPACES Guideline for Heliostat Performance Testing," Release 1.0, SolarPACES, https://elib.dlr.de/199045/
[14] sbp, 2022, "Kumul Dongfang Tower Stellio," sbp sonne, https://www.sbp.solar/project/kumul-dongfang-tower-stellio/?lang=en
[15] Téllez, F., Burisch, M., Cillasante, C., Sanchez, M., Sansom, C., Kirby, P., et al., 2014, "State of the Art in Heliostats and Definition of Specifications," STAGE-STE Project, Madrid.
[16] Ardani, K., Hunter, C., Johnson, C., and Koebrich, S., 2001, "Maximizing Solar and Transportation Synergies," National Renewable Energy Laboratory (NREL), Golden, CO, NREL/TP-6A20-80779, https://www.nrel.gov/docs/fy21osti/80779.pdf
[17] Kolb, G. J., Davenport, R., Gorman, D., Lumia, R., Thomas, R., and Donnelly, M., 2007, "Heliostat Cost Reduction," ASME 2007 Energy Sustainability Conference, pp. 1077–1084.
[18] National Renewable Energy Laboratory (NREL), "SolTrace," https://github.com/NREL/SolTrace
[19] Emes, M. J., Jafari, A., Ghanadi, F., and Arjomandi, M., 2019, "Hinge and Overturning Moments Due to Unsteady Heliostat Pressure Distributions in a Turbulent Atmospheric Boundary Layer," Sol. Energy, **193**(1), pp. 604–617.
[20] von Reeken, F., Weinrebe, G., Keck, T., and Balz, M., 2016, "Heliostat Cost Optimization Study," AIP Conf. Proc., **1734**(1), p. 160018.
[21] Potter, D. F., Kim, J.-S., Khassapov, A., Pascual, R., Hetherton, L., and Zhang, Z., 2018, "Heliosim: An Integrated Model for the Optimization and Simulation of Central Receiver CSP Facilities," Santiago, Chile, p. 210011.
[22] Pfahl, A., Coventry, J., Röger, M., Wolfertstetter, F., Vásquez-Arango, J. F., Gross, F., Arjomandi, M., Schwarzbözl, P., Geiger, M., and Liedke, P., 2017, "Progress in Heliostat Development," Sol. Energy, **152**(9), pp. 3–37.
[23] Pfahl, A., Randt, M., Holze, C., and Unterschütz, S., 2013, "Autonomous Light-Weight Heliostat With Rim Drives," Sol. Energy, **92**(1), pp. 230–240.
[24] Pfahl, A., and Uhlemann, H., 2011, "Wind Loads on Heliostats and Photovoltaic Trackers at Various Reynolds Numbers," J. Wind Eng. Ind. Aerodyn., **99**(9), pp. 964–968.
[25] Armstrong, P., and Izygon, M., 2014, "An Innovative Software for Analysis of Sun Position Algorithms," Energy Procedia, **49**(1), pp. 2444–2453.
[26] Kurup, P., Akar, S., Glynn, S., Augustine, C., and Davenport, P., 2022, "Cost Update: Commercial and Advanced Heliostat Collectors," NREL/TP-7A40-80482, 1847876, MainId:42685, https://www.nrel.gov/docs/fy22osti/80482.pdf
[27] Carrascosa, M. A., Blázquez, J. M., Calle, S. N. D. L., Sørensen, S. S., Falsig, J. J., Gallego, J. F., and Rodriguez, E., 2020, "High Quality Heliostats Leading to New Optimal Field Layouts Coupled With an Asymmetric Receiver Geometry," AIP Conf. Proc., **2303**(1), p. 030008.
[28] Cardoso, J. P., Mutuberria, A., Marakkos, C., Schoettl, P., Osório, T., and Les, I., 2018, "New Functionalities for the Tonatiuh Ray-Tracing Software," AIP Conf. Proc., **2033**(1), p. 210010.
[29] Ahlbrink, N., Belhomme, B., Flesch, R., Maldonado Quinto, D., Rong, A., and Schwarzbözl, P., 2012, "STRAL: Fast Ray Tracing Software With Tool Coupling Capabilities for High-Precision Simulations of Solar Thermal Power Plants," Proceedings of the SolarPACES 2012 Conference, Marrakesch, Marokko, https://elib.dlr.de/78440/, Accessed August 11, 2022.
[30] Wang, Y., and Pye, J., 2021, "Tracer 1.0.0," Australian National University Solar Thermal Group, https://github.com/anustg/Tracer
[31] Magdaleno López, C., Pérez Bueno, J. D. J., Cabello Mendez, J. A., Hernández Leos, R., Mendoza López, M. L., Sosa Domínguez, A., and Meas Vong, Y., 2022, "Deterioration of Novel Silver Coated Mirrors on Polycarbonate Used for Concentrated Solar Power," Sustainability, **14**(24), p. 16360.
[32] Kolb, G. J., Jones, S. A., Donnelly, M. W., Gorman, D., Thomas, R., Davenport, R., and Lumia, R., 2007, "Heliostat Cost Reduction Study," SAND2007-3293, 912923, Sandia National Laboratories.
[33] Meso-Star, 2021, "Solstice 0.9.1," https://www.meso-star.com/projects/solstice/solstice.html, Accessed August 25, 2022.
[34] Davidson, J. H., 2022, *Handbook of Solar Thermal Technologies: Principles and Applications*, Vol. 3, World Scientific, Singapore.
[35] Mammar, M., Djouimaa, S., Hamidat, A., Bahria, S., and El Ganaoui, M., 2017, "Wind Effect on Full-Scale Design of Heliostat with Torque Tube," Mech. Indus., **18**(3), p. 312.
[36] Benammar, S., and Tee, K. F., 2019, "Structural Reliability Analysis of a Heliostat Under Wind Load for Concentrating Solar Power," Sol. Energy, **181**(1), pp. 43–52.

[2]https://www.nrel.gov/docs/fy22osti/83041.pdf

[37] SolarPACES, 2001, "CSP Projects Around the World – SolarPACES," https://www.solarpaces.org/csp-technologies/csp-projects-around-the-world/
[38] Bender, W., 2013, "Final Technical Progress Report: Development of Low-Cost Suspension Heliostat; December 7, 2011–December 6, 2012," NREL/SR-5200-57611, 1068630, https://www.nrel.gov/docs/fy13osti/57611.pdf
[39] Sanchez, G., Serrano, A., Cancillo, M. L., and Garcia, J. A., 2015, "Pyranometer Thermal Offset: Measurement and Analysis," J. Atmos. Ocean. Technol., **32**(2), pp. 234–246.
[40] Pfahl, A., Coventry, J., Röger, M., Wolfertstetter, F., Vásquez-Arango, J. F., Gross, F., Arjomandi, M., Schwarzbözl, P., Geiger, M., and Liedke, P., 2017, "Progress in Heliostat Development," Sol. Energy, **152**(9), pp. 3–37.
[41] Pfahl, A., Randt, M., Holze, C., and Unterschütz, S., 2013, "Autonomous Light-Weight Heliostat With Rim Drives," Sol. Energy, **92**(1), pp. 230–240.
[42] Davila-Peralta, C., Rademacher, M., Emerson, N., Chavez-Lopez, G., Sosa, P., Cabanillas, R., Peon-Anaya, R., Flores-Montijo, N., Didato, N., and Angel, R., 2020, "Progress in Track-Mounted Heliostat," AIP Conf. Proc., **2303**(1), p. 030011.
[43] Kolb, G. J., Davenport, R., Gorman, D., Lumia, R., Thomas, R., and Donnelly, M., 2007, "Heliostat Cost Reduction," ASME 2007 Energy Sustainability Conference, pp. 1077–1084.
[44] Peterka, J. A. and Derickson, R. G., 1992, "Wind Load Design Methods for Ground-Based Heliostats and Parabolic Dish Collectors," SAND-92-7009, Sandia National Laboratories, Albuquerque, NM. https://www.osti.gov/biblio/7105290.
[45] Agarwal, N., Raj, M., and Bhattacharya, J., 2020, "Solar Tower on an Uneven Terrain: Methodology and Case Study," Renewable Energy, **161**(1), pp. 543–558.
[46] Coventry, J., Campbell, J., Xue, Y. P., Hall, C., Kim, J. S., Pye, J., Burgess, G., et al., 2016, "Heliostat Cost Down Scoping Study – Final Report," University of Tasmania Report.
[47] Little, C., Small, D., and Yelloowhair, J., 2021, "LiDAR For Heliostat Optical Error Assessment," Sandia National Laboratories, Albuquerque, NM, Report No. SAND2021-5956R.
[48] Sattler, J. C., Röger, M., Schwarzbözl, P., Buck, R., Macke, A., Raeder, C., and Göttsche, J., 2020, "Review of Heliostat Calibration and Tracking Control Methods," Sol. Energy, **207**(1), pp. 110–132.
[49] Burisch, M., Olano, X., Sanchez, M., Olarra, A., Villasante, C., Olasolo, D., Monterreal, R., Enrique, R., and Fernández, J., 2018, "Scalable Heliostat Calibration System (SHORT)—Calibrate a Whole Heliostat Field in a Single Night," AIP Conf. Proc., **2033**(2), p. 040009.
[50] Minis, N., Rosenbluth, E., Hayut, R., and Am-Shallem, M., 2019, "Spatial DNI Measurement for Accurate Solar Flux Control in Megalim 121 MWe Solar Receiver Power Plant," 24th SolarPACES 2019, Casablanca, Morocco.
[51] Blume, K., Röger, M., Schlichting, T., Macke, A., and Pitz-Paal, R., 2020, "Dynamic Photogrammetry Applied to a Real Scale Heliostat: Insights Into the Wind-Induced Behavior and Effects on the Optical Performance," Sol. Energy, **212**(2), pp. 297–308.
[52] Pottler, K., Lupfert, E., Johnston, G. H., and Shortis, M. R., 2005, "Photogrammetry: A Powerful Tool for Geometric Analysis of Solar Concentrators and Their Components," ASME J. Sol. Energy Eng., **127**(1), pp. 94–101.
[53] Röger, M., Prahl, C., and Ulmer, S., 2008, "Fast Determination of Heliostat Shape and Orientation by Edge Detection and Photogrammetry," 14th SolarPACES 2008, Las Vegas, NV.
[54] Shortis, M. R., and Johnston, G. H. G., 1996, "Photogrammetry: An Available Surface Characterization Tool for Solar Concentrators, Part I: Measurements of Surfaces," ASME J. Sol. Energy Eng., **118**(3), pp. 146–150.
[55] Burke, J., Li, W., Heimsath, A., von Kopylow, C., and Bergmann, R. B., 2013, , "Qualifying Parabolic Mirrors with Deflectometry," J. Eur. Opt. Soc. Rapid Publ., **8**, p. 13014.
[56] Montecchi, M., Cara, G., and Benedetti, A., 2020, "VISproLF: Self-Calibrating Instrument for Measuring 3D Shape of Linear Fresnel Facets," Rev. Sci. Instrum., **91**(8), p. 083109.
[57] Hanrieder, N., Sengupta, M., Xie, Y., Wilbert, S., and Pitz-Paal, R., 2016, "Modeling Beam Attenuation in Solar Tower Plants Using Common DNI Measurements," Sol. Energy, **129**(1), pp. 244–255.
[58] Sánchez, M., Fernández-Peruchena, C. M., Bernardos, A., Heras, C., Chueca, R., and Salinas, I., 2019, "High-Accuracy Real-Time Monitoring of Solar Radiation Attenuation in Commercial Solar Towers," 24th SolarPACES 2019, Casablanca, Morocco.
[59] Sattler, J. C., Röger, M., Schwarzbözl, P., Buck, R., Macke, A., Raeder, C., and Göttsche, J., 2020, "Review of Heliostat Calibration and Tracking Control Methods," Sol. Energy, **207**(1), pp. 110–132.
[60] Malan, K. J., 2014, "A Heliostat Field Control System," Doctoral dissertation, Stellenbosch University.
[61] Swart, B. D., 2017, "A Method for Accurate Measurement of Heliostat Mirror Orientation," Doctoral dissertation, Stellenbosch University.
[62] Hanrieder, N., Wilbert, S., Pitz-Paal, R., Emde, C., Gasteiger, J., Mayer, B., and Polo, J., 2015, "Atmospheric Extinction in Solar Tower Plants: Absorption and Broadband Correction for MOR Measurements," Atmos. Meas. Tech., **8**(8), pp. 3467–3480.
[63] Fernández García, A., 2021, "Soiling Measurements of Solar Reflectors: Portable Reflectometers to Measure Soiled Reflectors in Solar Fields," SolarPACES Task III Solar Technology and Advanced Applications Report, SolarPACES, https://www.solarpaces.org/wp-content/uploads/Document-2_SolarPACES_Portable-Reflectometers.pdf
[64] Glatzmaier, G., Wendelin, T., and Zhu, G., 2014, "Multi-Heliostat Wireless Communication Assessment," National Renewable Energy Laboratory, NREL_25830.
[65] Alami Merrouni, A., Conceição, R., Mouaky, A., Silva, H. G., and Ghennioui, A., 2020, "CSP Performance and Yield Analysis Including Soiling Measurements for Morocco and Portugal," Renewable Energy, **162**(1), pp. 1777–1792.
[66] Collares, M., 2014, "State of the Art in Heliostats and Definition of Specifications," STAGE-STE Project, EERA Report 2014.
[67] Amsbeck, L., Buck, R., Pfahl, A., and Uhlig, R., 2008, "Optical Performance and Weight Estimation of a Heliostat with Ganged Facets," ASME J. Sol. Energy Eng., **130**(1), p. 011010.
[68] Relloso, S., and Gutiérrez, Y., 2017, "SENER Molten Salt Tower Technology. Ouarzazate NOOR III Case," 22nd SolarPACES 2017, SolarPACES, AIP Conference Proceedings, Abu Dhabi, United Arab Emirates.
[69] Emes, M., Yellapantula, S., Sment, J., Armijo, K., Muller, M., Mehos, M., Brost, R., and Arjomandi, M., 2024, "Heliostat Consortium: Gap Analysis on State of the Art in Wind Load Design," ASME J. Sol. Energy Eng., **146**(6), p. 061001.
[70] Nudehi, S. S., Duncan, G. S., and Venstrom, L. J., 2019, "Heliostat Attitude Control Strategy in the Solar Energy Research Facility of Valparaiso University," ASME J. Sol. Energy Eng., **141**(5), p. 051005.